Original Article

Initial Stress Differences Between Sliding and Sectional Mechanics with an Endosseous Implant as Anchorage: A 3-Dimensional Finite Element Analysis

Mónica Vásquez, DDS[a]; Eliana Calao, DDS, MS[b]; Fabio Becerra, DDS, Certificate in Periodontics[c]; Jorge Ossa, DDS, MS[d]; Carlos Enríquez, MS Computer Science, MS Experimental Stress Analysis[e]; Eliseo Fresneda, MS Machinery Design[f]

Abstract: Endosseous implants have been used as orthodontic anchorage in recent years. A 3-dimensional mathematical model was constructed that uses the finite element method, which simulated an endosseous implant and an upper canine with its periodontal ligament and cortical and cancellous bone. Levels of initial stress were measured during 2 types of canine retraction mechanics (friction and frictionless). The lower magnitude and more uniform stresses in the implant and its cortical bone were found to have a moment-force ratio (M/F) of 6.1:1, whereas the canine and its supporting structures exerted a M/F ratio of 10.3:1. On the basis of these results, when the anchor unit is an endosseous implant, it seems better to use a precalibrated retraction system without friction (T-loop) where a low load-deflection curve would be generated. (*Angle Orthod* 2001;71:247–256.)

Key Words: Endosseous implant; Moment-force ratio; Stress; Finite element method

INTRODUCTION

Orthodontic anchorage provided by teeth or extraoral structures is used to resist undesirable tooth movement or reaction forces. Adequate anchorage may become difficult, if not impossible, to obtain when teeth are missing. Such cases would benefit from an anchor unit, such as an implant, which could receive forces of enough magnitude to produce movement without becoming displaced by the applied forces.[1]

Since the introduction of osseointegration, titanium implants have been used successfully in the clinical treatment of edentulous patients. In addition to the prosthetic application of endosseous implants, considerable interest has developed in their use as an anchorage system in orthodontics and dentofacial orthopedics.[2] Their application under orthodontic forces has been demonstrated both clinically[2–6] and experimentally.[1,7–11]

Orthodontic tooth movement during space closure is achieved through 2 types of mechanics. The first type, frictionless, involves closing loops fabricated either in full or sectional arch wires. The teeth move because of the activation of the wire loop, which can be designed to provide a low load-deflection curve and a controlled moment to force ratio (M/F). The second type—sliding, or frictional, mechanics—involves either moving teeth along an arch wire or sliding the arch wire through brackets and tubes.[12,13]

Elastomeric chains are extensively used in orthodontics to apply forces for canine retraction with frictional mechanics. One of its characteristics is the inability to deliver a continuous force level over an extended period of time. In 1970, Andreasen and Bishara[14] demonstrated that after 24 hours of activation, Alastik modules (Unitek, Monrovia, Calif) lose up to 74% of their force. In 1975, Hershey and Reynolds,[15] in contrast with Andreasen and Bishara,[14] found a 50% force loss after the first day, with 40% of the original force remaining after 4 weeks. In order to compensate for the high and rapid decay rates of elastomers, initial forces must often be 4 times greater than that which is desirable.[14]

Traditional stress analytical experimental methods, such

[a] Private practice orthodontist, Medellín, Colombia.
[b] Private practice orthodontist, Medellín, Colombia.
[c] Titular and Distinguished Professor, Universidad de Antioquia. Medellín, Colombia.
[d] Orthodontist, Associate Professor, University of Antioquia, Medellín, Colombia.
[e] Mechanical Engineer, Associate Professor, National University, Medellín, Colombia.
[f] Mechanical Engineer, Associate Professor, National University, Medellín, Colombia.
Corresponding author: Mónica Lena Vásquez, Calle 12 C Sur # 39–153. Edificio la gruta del poblado, bloque 1, apto 903, Medellín, Colombia, South América.
(e-mail: vasquezgomez@epm.net.co).

Accepted: October 2000. Submitted: May 2000.

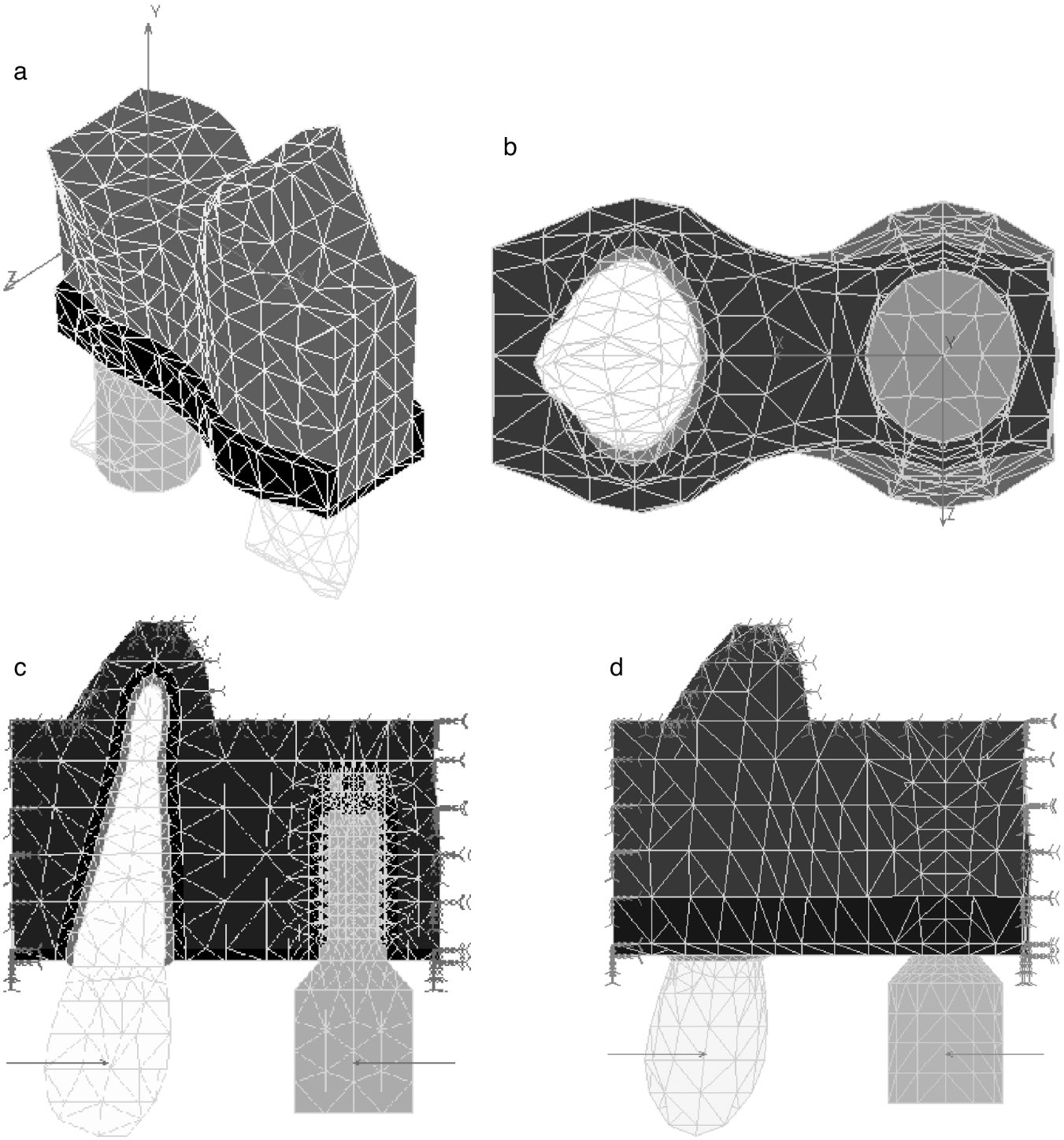

FIGURE 1. Finite element model. 1a: Buccal view; 1b: Occlusal view, 1c: Mesio-distal view (internal) and 1d: Mesio-distal view (from buccal).

as photoelasticity, interferometric holography, and strain gauges, have been reported in dental stress analyses.[16,17] The finite element method (FEM), a modern tool of numerical stress analytical technique, has the advantage of being applicable to solids of irregular geometry that contain heterogeneous material properties. It is, therefore, ideally suited to evaluate the structural behavior of teeth.[18]

FEM provides the orthodontist with quantitative data that can extend the understanding of the physiologic reactions that occur within the dentoalveolar complex.[19] More specifically, such numerical techniques may yield an improved understanding of the reactions and interactions of individual tissues.[20] Such detailed information of the stresses and strains is difficult to obtain and analyze by other experi-

TABLE 1. Model Dimensions[a]

Implant	Nucleus	Transmucosus Post	Screw Pass
Diameter	3.75 mm	7.0 mm	
Length	10 mm	8.0 mm	0.6 mm
Cuspid	Length	Maximum mesiodistal diameter	Maximum mesiodistal diameter
Crown	10 mm	7.4 mm	7.3 mm
Root	15 mm	5.5 mm	7.8 mm
Supporting Structures	Bone		Periodontal ligament
	Lamellar bone	Cortical bone	
Diameter	0.7 mm	1.0 mm	0.35 mm

[a] From *Lifecore Catalog,*[22] Krause et al,[23] and Lindhe.[24]

TABLE 2. Mechanical Properties for the Titanium, Tooth, Periodontal Ligament (PDL), and Cortical and Alveolar Bone[a]

Material	Young's Modulus, N/mm^2	Poisson's Ratio, N/mm^2
Titanium	1.10E + 05	3.0E − 01
Cortical bone	1.37E + 04	2.6E − 01
Cancellous bone	1.37E + 03	3.0E − 01
PDL	6.67E − 01	4.5E − 01
Dentin (tooth)	1.96E + 04	3.0E − 01

[a] From Middleton et al,[19] Tonne, et al,[20] McGuiness et al,[21] Rieger et al,[25] Van Rosen et al,[26] and Meijer et al.[27]

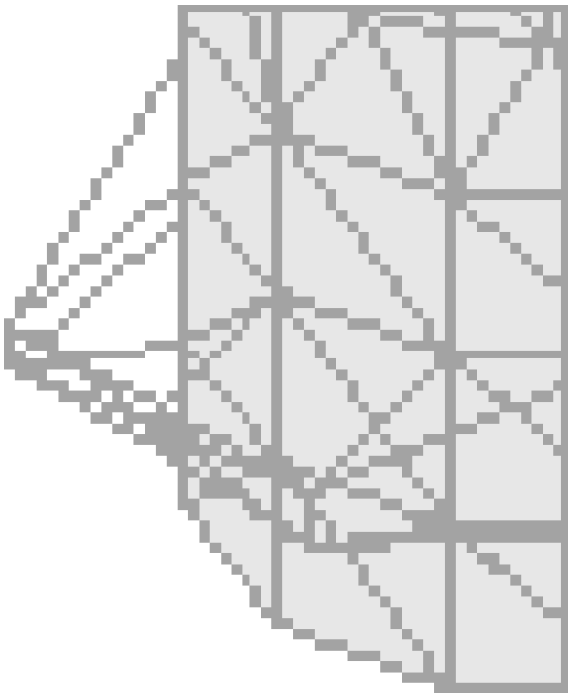

FIGURE 2. Rigid structure to simulate the bracket slot and the tube.

mental techniques because of the interaction with the surrounding tissues.[21]

The purpose of this study was, therefore, to determine and compare the initial stress profiles in an upper cuspid, an endosseous implant, and their supporting structures with

TABLE 3. Point of Force Application

Variable	Bracket of the Cuspid	Tube of the Implant
Occluso-gingival height	4.5 mm	2.5 mm
Buccal-lingual separation	1.7 mm	1.7 mm
Slot	0.018 × 0.025 inch	0.018 × 0.025 inch

TABLE 4. Force Application (Force and Moments)[a]

Load Condition	Force or Moment Magnitude[c]	Sense[b]		Retraction Mechanics	Activation
		Cuspid	Implant		
1	1.96 N	+	−	Elastic chain	
2	4.9 N	+	−	Elastic chain	
3	3.37 N	+	−	T loop (TMA)	6 mm
4	20.6 N/mm	−	+	T loop (TMA)	6 mm
5	1.67 N	+	−	T loop (TMA)	3 mm
6	17.25 N/mm	−	+	T loop (TMA)	3 mm
7	1.13 N	+	−	T loop (TMA)	2 mm
8	15.67 N/mm	−	+	T loop (TMA)	2 mm
9	0.53 N	+	−	T loop (TMA)	1 mm
10	13.9 N/mm	−	+	T loop (TMA)	1 mm

[a] From Kuhlberg and Burstone.

[b] Force: + indicates distal crown movement; −, mesial movement of transmucosal post. Moment: + indicates mesial implant movement; −, distal root movement.

[c] Newton System (kilogram, meter, second) 1 N (N) = 102 grams.

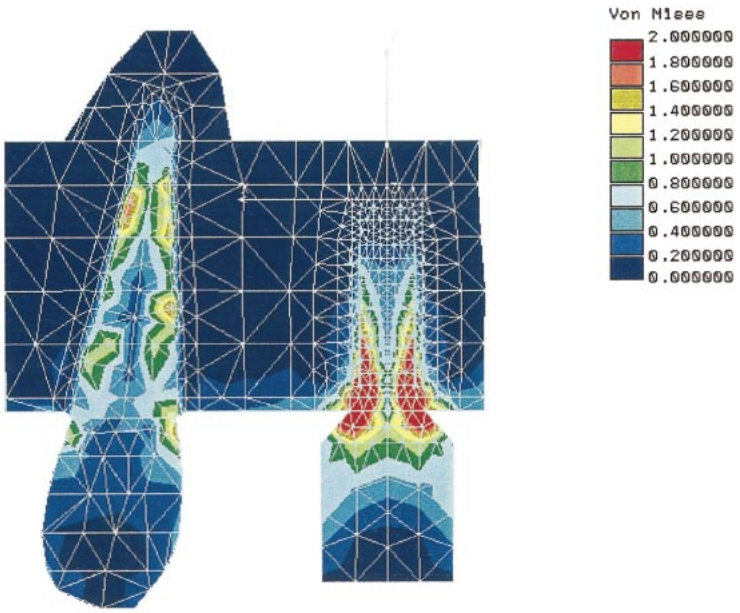

FIGURE 3. Von Misses stresses in load 2 (4.9 N). Colors indicate the magnitude of the stresses.

different moments and forces (simulating canine retraction with elastic chains and T-loops) by using the FEM.

MATERIALS AND METHODS

A 3-dimensional, orthogonal, Cartesian model was generated by using the COSMOS/M 1.75 of 64,000 nodes software system. The model was composed of a Branemark endosseous titanium implant with standard dimensions; the implant simulated the position of an upper first permanent molar and an upper cuspid of average size, with periodontal ligament (PDL) and cortical and cancellous bone (Table 1; Figure 1).

The model was divided into 14,953 nodes and 34,109 elements: all of them were tetra 4-R type, a solid element with 4 faces and 4 nodes. Each node had 6 degrees of freedom—3 rotations and 3 translations. Homogeneous, isotropic, and linearly elastic behavior was assumed for all the materials (Table 2). Boundary conditions were located at the floor of the nasal cavity and maxillary sinus and at the lateral surface of the maxillary bone (Figure 1c and d).

To apply the forces, 2 rigid structures simulating the bracket slot and the tube were modeled (Table 3; Figure 2). In the center of each rigid structure, 14 different forces were applied in a mesio-distal direction: the first 2 simulated the retraction of the upper cuspid with elastic chains.[14,28] The other 12 simulated the retraction by a segmented 0.017 × 0.025 inch T-loop in a TMA wire (Ormco Corporation, Glendora, Calif) designed to produce equal and opposite moments when the loop is in the centered position[29,30] (Tables 4 and 5).

The stresses and deflections were determined at different mesio-distal and occluso-gingival levels. In addition, specific stress values were evaluated in the different nodes of the root surface, PDL, cortical bone, and implant from the apical zone to the cervical margin.

Results were expressed as Von Misses stresses (combined effect of the different stresses) and compressive and tensile stress in the x- and y-axes. Principal stresses—maximum (P_1), intermediate (P_2), and minimum (P_3)—were evaluated, but they were similar in shape and magnitude to the stresses examined in the x- and y-axes (P_1 stresses were mostly tensile, P_3 were compressive, and P_2 were an intermediate value between P_1 and P_2).

RESULTS

The behavior of the evaluated structures under single forces or moments were linearly or directly proportional to the applied load. To simplify the analysis, loads 2 and 4, which corresponded to the maximum force and moment, and the combined loads 51, 56, 78, and 91 with different M/F ratios were evaluated (Tables 4 and 5).

Von Misses stresses in the evaluated loads showed the highest stresses on the implant and the cortical bone at the cervical third. The lowest stresses appeared at the apical third of the implant. By structure, the highest stress was observed in the implant, followed by the cuspid, the cortical bone, and finally, the periodontal ligament (Figure 3). Stress magnitudes were higher with a single force or moment than when the combined loads with different M/F ratio were considered.

The root, the implant, and its cortical bone exhibit large bending stresses in the y-axis (Figures 4–6). The implant behaved as a rigid structure, with the highest stresses concentrated in the first cervical screw, declining steadily to

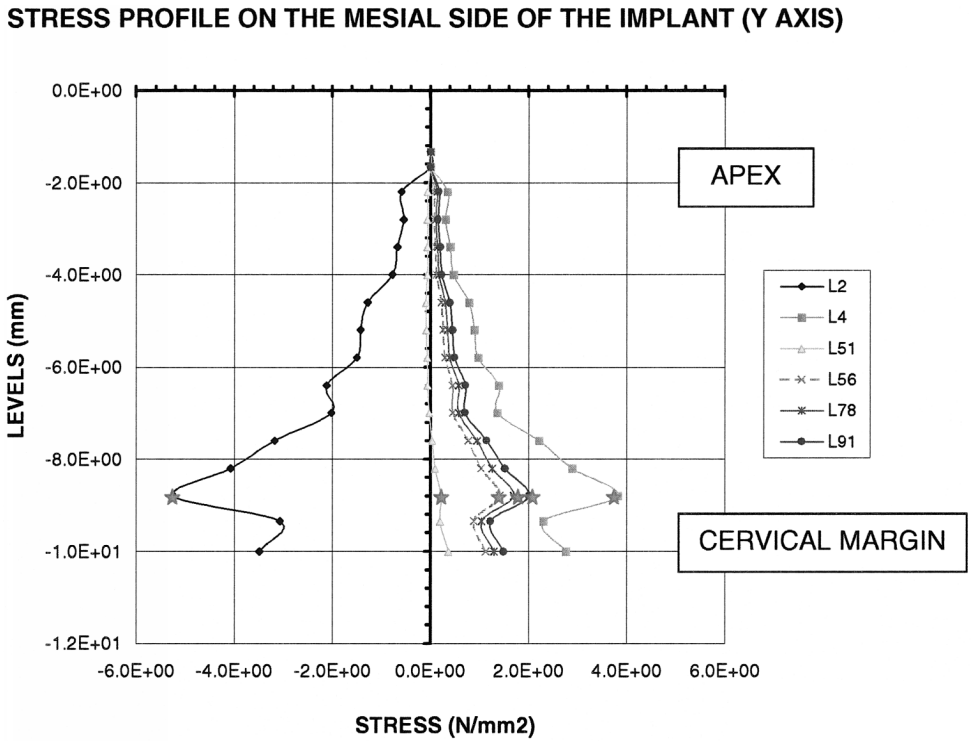

FIGURE 4. L2 = 4.9 N, L4 = 20.6 Nmm, L51 = Rel. M/F: 6.1:1, L56 = Rel. M/F: 10.1:1, L78 = Rel. M/F: 13.9:1, L91 = Rel. M/F: 26.4:1. Negative signs: Compressive stresses. Positive signs: Tensile stresses. Star: First screw node.

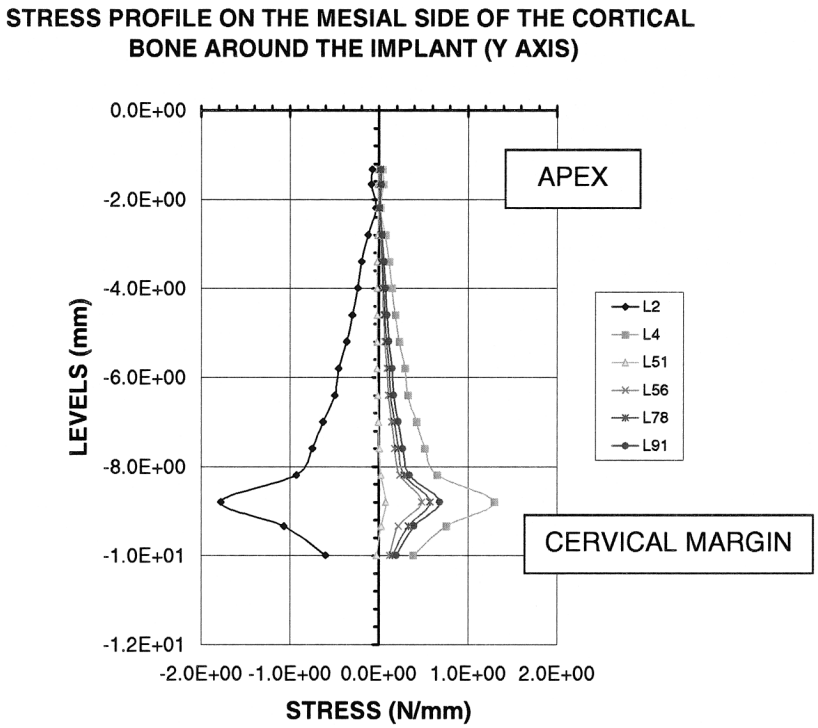

FIGURE 5. L2 = 4.9 N, L4 = 20.6 Nmm, L51 = Rel. M/F: 6.1:1, L56 = Rel. M/F: 10.1:1, L78 = Rel. M/F: 13.9:1, L91 = Rel. M/F: 26.4:1. Negative signs: Compressive stresses. Positive signs: Tensile stresses.

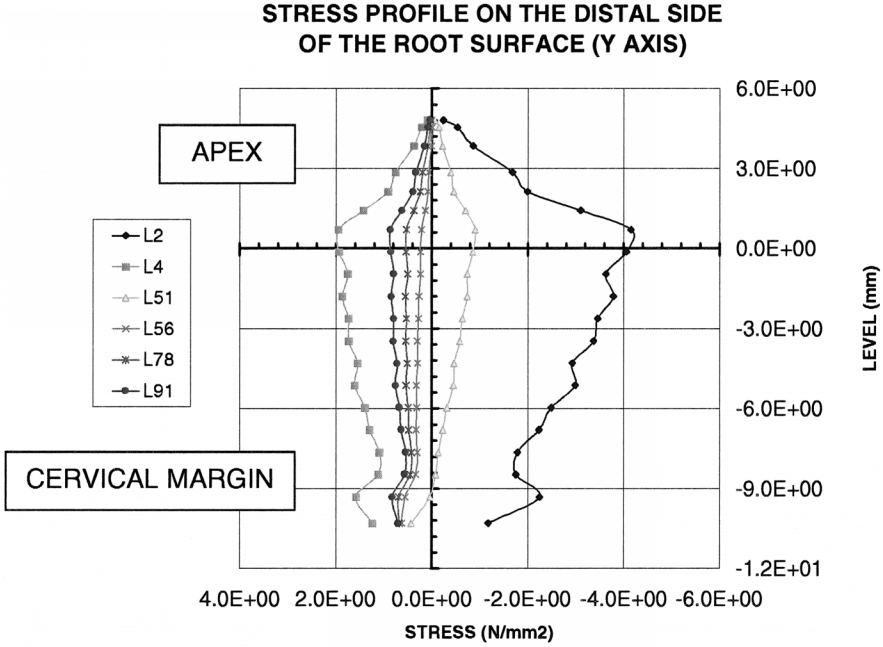

FIGURE 6. L2 = 4.9 N, L4 = 20.6 Nmm, L51 = Rel. M/F: 6.1:1, L56 = Rel. M/F: 10.1:1, L78 = Rel. M/F: 13.9:1, L91 = Rel. M/F: 26.4:1. Negative signs: Compressive stresses. Positive signs: Tensile stresses.

TABLE 5. Combined Force Application (Moment-Force Ratio)[a]

Load Condition[b]	Force Magnitude	Moment Magnitude	Moment-Force Ratio	Activation
51	3.37 N	20.6 N/mm	6.1	6 mm
56	1.67 N	17.25 N/mm	10.1	3 mm
78	1.13 N	15.67 N/mm	13.9	2 mm
91	0.53 N	13.9 N/mm	26.4	1 mm

[a] From Kuhlberg and Burstone.[30]

[b] Load 51 = the sum of load 3 and 4; Load 56 = the sum of load 5 and 6; Load 78 = the sum of load 7 and 8; and Load 91 = the sum of load 9 and 10.

the apex. On the other hand, at the canine, the highest stresses were found between the middle and the apical third, with a gradual reduction to approximately 0 at the cervical margin and at the apex. This could be caused by the differences in rigidity between the titanium and the dentin.

In Figures 4, 5, and 6, load 2 (4.9 N) produced compression, whereas the single moment (load 4; 20.6 N/mm) produced tension. Low stress magnitudes were seen in the different moment-force ratios analyzed. In load 51 (moment-force ratio of 6.1:1), the single force profile predominated, whereas in loads 56, 78, and 91, moment effects prevailed (Tables 4 and 5). Stress distribution on the mesial and distal sides showed almost symmetrical, but opposite, behavior.

Evaluation of the x-axis on the cortical bone around the implant revealed that the cervical margin and the bone around the first screw of the implant were the major stress points (Figure 7).

An analysis of the structures showed that the PDL presented the least stress magnitude, having a similar pattern of stress distribution at both in the PDL-tooth and PDL-bone interfaces and on the x- and y-axes. At the same time, stress distributions for the PDL and lamellar bone were similar, although lamellar bone stresses were of greater magnitude and had a more irregular distribution (Figures 8 and 9). To establish a relation between stresses and displacements (Figure 10), the analysis was done on the x-axis.

Stress curves of the PDL cross the vertical axis, representing the center of rotation during tooth movement. This area showing 0 stresses varies with the different moment-force ratios and with the type of movement (Figures 8 and 10; Table 6). The stress profiles for the evaluated loads in the mesial side of the root surface, PDL, and cortical bone were similar but opposite in sign.

DISCUSSION

One of the remodeling theories argues that local mechanical signals stimulate or induce regulating cells to trigger remodeling events.[35] This implies the importance of studying stress levels from orthodontic forces in the root surface, PDL, and cortical bone and those that occur in the anchor unit like bones, or, as in this case, in an osseointegrated implant.

Overall, the highest stresses occurred in the implant, followed by the canine root surface and cortical bone and finally, the PDL (Figure 3). This could have been caused by the geometric differences and the different mechanical

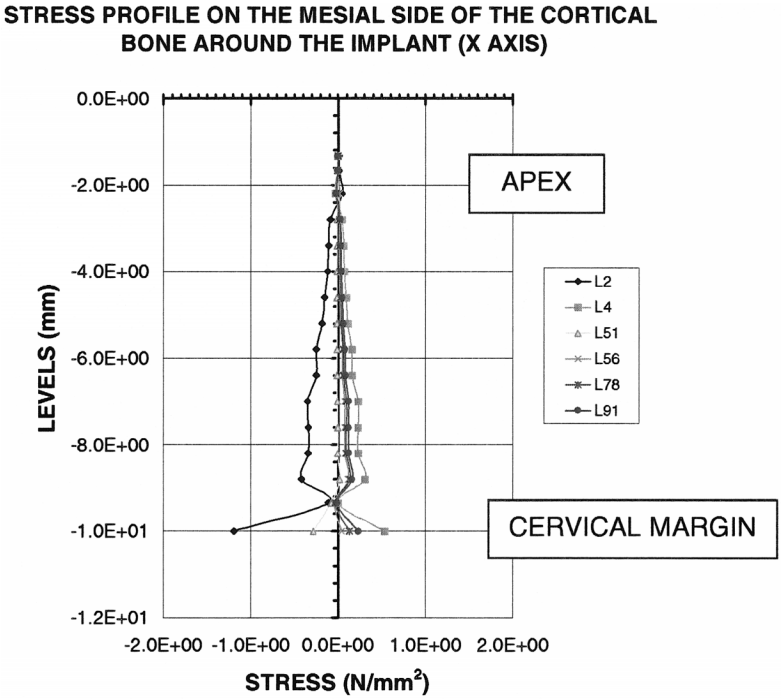

FIGURE 7. L2 = 4.9 N, L4 = 20.6 Nmm, L51 = Rel. M/F: 6.1:1, L56 = Rel. M/F: 10.1:1, L78 = Rel. M/F: 13.9:1, L91 = Rel. M/F: 26.4:1. Negative signs: Compressive stresses. Positive signs: Tensile stresses.

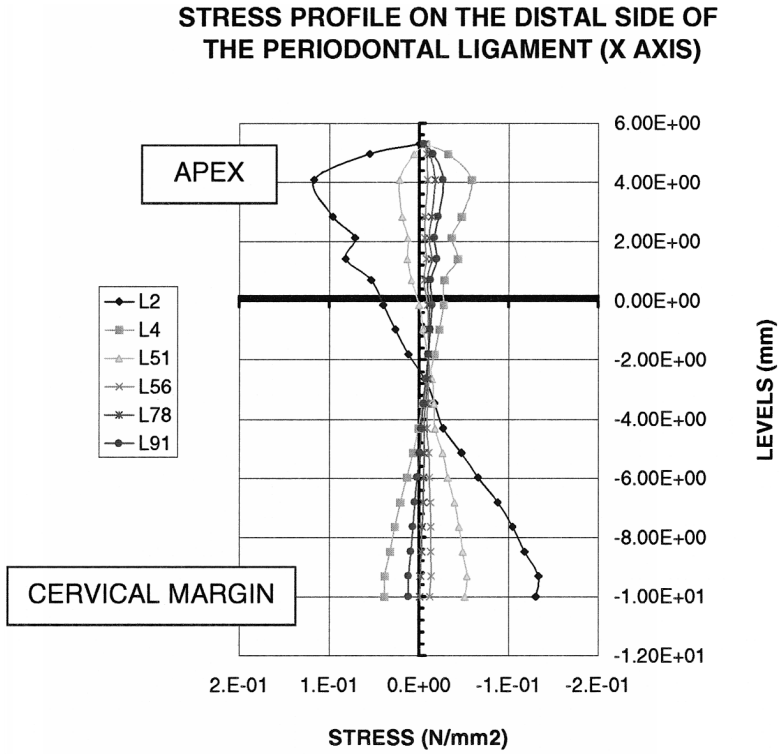

FIGURE 8. L2 = 4.9 N, L4 = 20.6 Nmm, L51 = Rel. M/F: 6.1:1, L56 = Rel. M/F: 10.1:1, L78 = Rel. M/F: 13.9:1, L91 = Rel. M/F: 26.4:1. Negative signs: Compressive stresses. Positive signs: Tensile stresses.

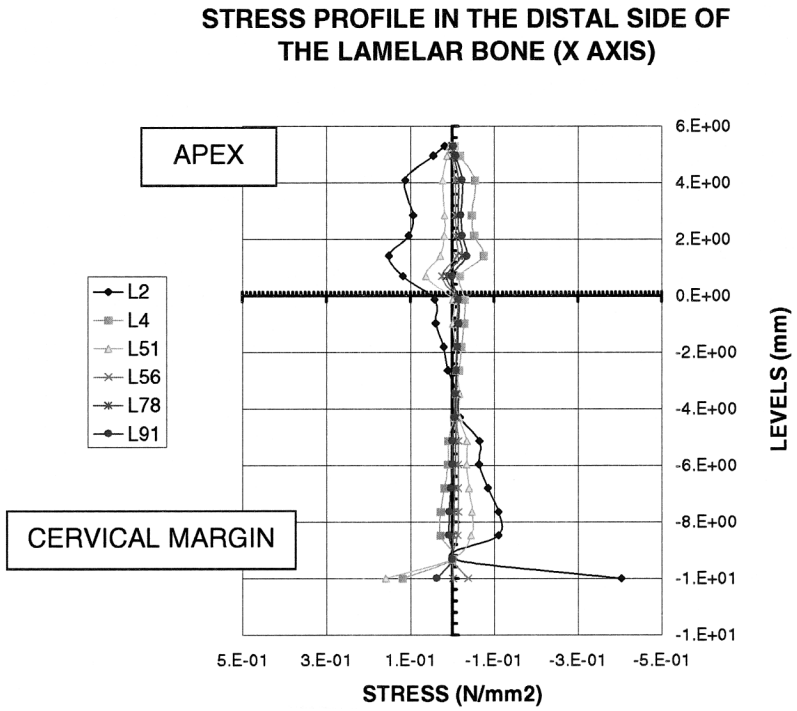

FIGURE 9. L2 = 4.9 N, L4 = 20.6 Nmm, L51 = Rel. M/F: 6.1:1, L56 = Rel. M/F: 10.1:1, L78 = Rel. M/F: 13.9:1, L91 = Rel. M/F: 26.4:1. Negative signs: Compressive stresses. Positive signs: Tensile stresses.

TABLE 6. Periodontal Ligament Stresses and Displacements (Distal Side) in the X-Axis for Different Loads

Load Force or M/F	Load 2 4.9 N	Load 4 20.6 N	Load 51 6.1:1	Load 56 10.3:1	Load 78 13.9:1	Load 91 26.4:1
Stress						
Compressive	Cervical	Apical	Cervical of low magnitude	From the cervical margin to the apex of low magnitude	Low magnitude, increasing progressively from the cervical margin to the apex	Apical of low magnitude
Tensile	Apical	Cervical	Apical of low magnitude	…	…	Cervical of low magnitude
Type of movement	Uncontrolled tipping of the crown to distal	Uncontrolled tipping of the crown to mesial	Uncontrolled tipping of the crown to distal	Translation	Uncontrolled tipping of the crown to mesial	Uncontrolled tipping of the crown to mesial
Center of rotation or point of 0 stress	7.5 mm apically from the cervical margin	6.0 mm apically from the cervical margin	9.0 mm apically from the cervical margin	No point	Cervical margin	5.0 mm apically from the cervical margin

properties of the implant, tooth, cortical bone, and PDL. In 3-dimensional FEM studies, Tanne et al[20] and Puente et al[31] reported the same distribution, with the exception that the osseointegrated implant that was not modeled.

The highest stress concentration in the implant was localized in the cervical margin and at the first screw (1.2 mm apically from the cervical margin). Similar findings had been presented by Meijer et al,[27] Barbier et al,[32] and Clelland et al.[33] However, it is important to point out that these stresses are of such low magnitude that they are unable to produce a failure in the implant. Therefore, the osseointegrated implants are able to withstand orthodontic forces and may function as adequate anchor units. Their stress magnitude and distribution are better when a force and a moment are applied together (Figure 4).

Thus, in osseointegrated implants designed to serve as orthodontic anchors, the functional and structural union of titanium to the cervical bone should be free of bacterial plaque accumulation because this preserves cervical osseointegration (Figures 5 and 7).

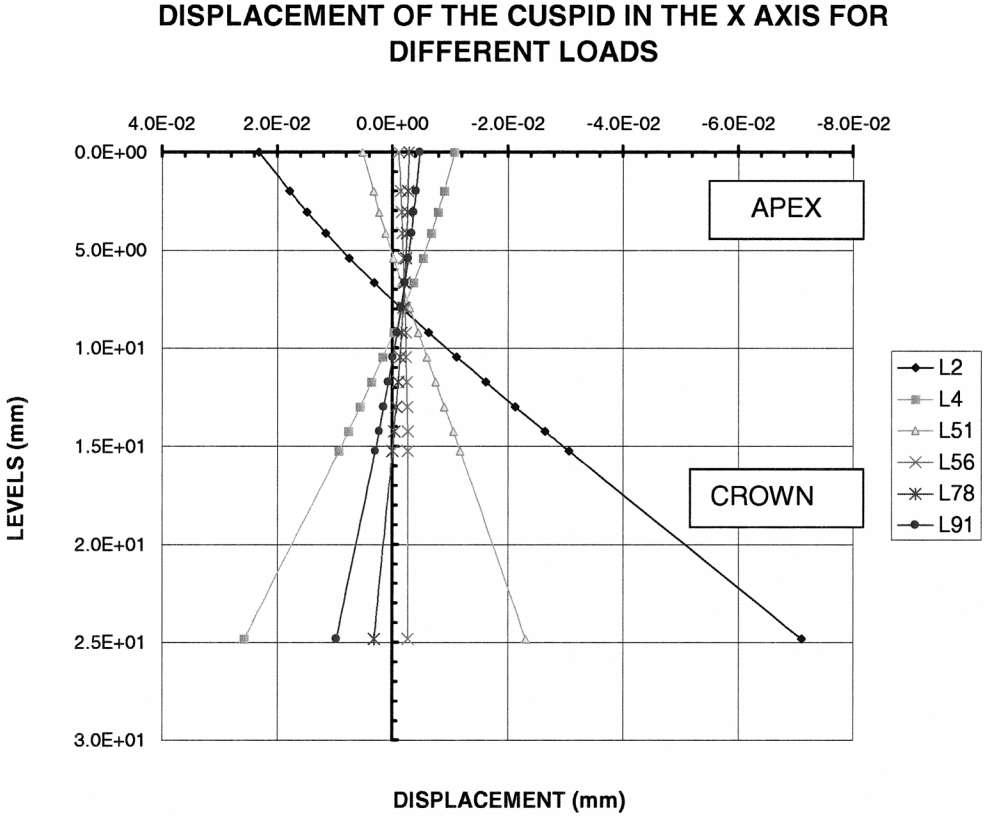

FIGURE 10. L2 = 4.9 N, L4 = 20.6 Nmm, L51 = Rel. M/F: 6.1:1, L56 = Rel. M/F: 10.1:1, L78 = Rel. M/F: 13.9:1, L91 = Rel. M/F: 26.4:1. Positive displacement: Mesial side. Negtative displacement: Distal side.

Large bending stresses were observed in the canine root surface, but not in the PDL. Tanne et al[20] found similar types of stresses at the surface of the root and at the alveolar bone. The differences found could be because they did not model the cortical bone (Figure 6).

A simple horizontal force produces tipping of the tooth, with its stress concentrated at the cervical margin and at the apex of the tooth. This force produced an area of zero stresses in the PDL and its cortical bone near the middle of the root (center of rotation).[20,21,31] This result agrees with the histologic findings that show that the cell-free area and hyalinization of the PDL are typically induced at the cervical and apical zones,[34] which are high-stress concentration sites. A single moment produced a similar tipping of the tooth, but in an opposite direction (Figures 8 and 10; Table 6).

There was a lower magnitude and more uniform stress distribution when the moment and force were applied together. The stress produced in the periodontal ligament was related to the tooth movement (Table 6). The M/F ratio of 6.1:1 induced an uncontrolled tipping of the tooth (with distal crown and mesial root movement), whereas the M/F ratio of 10.3:1 produced a translation movement, and the bending stresses were significantly reduced in magnitude (Figure 6). The stresses in the PDL were compressive and more constant in the translation movements than in the tipping ones (Figures 8 and 10), making the first more physiologic.[20]

When the M/F ratio increased to 13.9:1 or to 26.4:1, uncontrolled root movement with a mesial displacement of the crown was observed (Figure 10). The M/F ratio determined the type of movement and its center of rotation. Burstone et al[36] described similar findings.

During tooth movement, nonlinear elastic, plastic, and viscoelastic phenomena can occur.[34] In this article, only linear elastic behaviors of the tooth-periodontal structures are considered.[20,35] Therefore, in the future, additional modeling may be needed along with nonlinear elastic analysis.[20,35] However, the model does provide quantitative results of the complex 3-dimensional stresses caused by mesio-distal forces during orthodontic treatment. The model allows areas of high stress to be accurately located, and these are considered to be relevant in understanding the long-term behavior of orthodontic tooth movement.[35]

CONCLUSIONS

Overall, the area with the highest stress was the cervical margin of the osseointegrated implant and its cortical bone. These stresses are of such low magnitude that they are unable to produce a permanent failure of the implant. Large

bending stresses were found along the surface of the canine and at the implant.

Stress distribution was similar in the PDL and in the cortical bone around the canine, with a larger magnitude and more irregular stress distribution in the cortical bone. The zero-stress area is associated with the center of rotation of the tooth, which varies with the different moment-force ratios and with the type of movement.

The combined loads with different M/F ratios produced the lower and more uniform stress distribution. The M/F ratio 6.1:1 had the best stress distribution in the implant and its cortical bone. The same was observed in the canine and its supporting structures with a M/F ratio of 10.3:1. Then, when the anchor unit is an endosseous implant, it is better to use a precalibrated retraction system without friction (T-loop) and with a low load-deflection curve in which the M/F ratio is known.

In the future, when the cell reaction to variable stress levels is known for each structure in the stomatognathic system, studies like this will have a big influence in clinical orthodontics.

ACKNOWLEDGMENT

We would like to acknowledge engineers Carlos Enriquez G. and Eliseo Fresneda B. for their technical assistance. This work was supported by the CODI Faculty of Dentistry, University of Antioquia.

REFERENCES

1. Turley PK, Kean C, Schur J, Stefanac J, Gray J, Hennes J, Poon LC. Orthodontic force application to titanium endosseous implants. *Angle Orthod.* 1988;58:151–162.
2. Van Roekel NB. The use of Branemark system implants for orthodontic anchorage: report of a case. *Int J Oral Maxillofac Implants.* 1989;4:341–344.
3. Creekmore TB, Eklund MK. The possibility of skeletal anchorage. *J Clin Orthod.* 1983;17:266–269.
4. Roberts WE, Marshall KJ, Moszary PG. Rigid endosseous implant utilized as anchorage to protract molars and close an atrophic extraction site. *Angle Orthod.* 1990;60:135–152.
5. Higuchi KU, Slack JM. The use of titanium fixtures for intraoral anchorage to facilitate orthodontic tooth movement. *Int J Oral Maxillofac Implants.* 1991;6:338–344.
6. Wehrbein H, Merz BR, Diedrich P, Glatzmaier J. The use of palatal implants for orthodontic anchorage. *Clin Oral Implant Res.* 1996;7:410–416.
7. Gray JE, Steen ME, King GJ, Clark AE. Studies on the efficacy of implants as orthodontic anchorage. *Am J Orthod.* 1983;83:311–317.
8. Wehrbein H, Diedrich P. Endosseous titanium implants during and after orthodontic load: an experimental study in the dog. *Clin Oral Implant Res.* 1993;4:76–82.
9. Roberts WE, Smith RK, Ziberman Y, Mozsary PG, Smith RS. Osseous adaptation to continuous loading of rigid endosseous implants. *Am J Orthod.* 1984;86:95–110.
10. Smalley WM, Shapiro PA, Hohi TH, Kokich VG, Branemark P. Osseointegrated titanium for maxillofacial protraction in monkeys. *Am J Orthod Dentofacial Orthop.* 1988;94:285–295.
11. Block MS, Hoffman DR. A new device for absolute anchorage for orthodontics. *Am J Orthod Dentofacial Orthop.* 1995;107: 251–258.
12. Ziegler P, Ingervall B. Optimizing anterior and canine retraction. *Am J Orthod Dentofacial Orthop.* 1989;95:95–99.
13. Nanda R. *Biomechanics in Clinical Orthodontics.* Philadelphia, Pa: WB Saunders Co; 1997:188.
14. Andreasen GF, Bishara S. A comparison of the time related forces between plastic elastics and latex elastics. *Angle Orthod.* 1970; 40:319–328.
15. Hersey HG, Reynolds WG. The plastic module as an orthodontic tooth-moving mechanism. *Am J Orthod.* 1975;67:554–562.
16. Mahler DB, Peyton FA. Photoelasticity as a research technique for analyzing stresses in dental structures. *J Dent Res.* 1955;34: 831–838.
17. Andersen KL, Pedersen EH, Melsen B. Material parameters and stress profiles within the periodontal ligament. *Am J Orthod Dentofacial Orthop.* 1991;99:427–444.
18. Yettram AL, Wright KW, Pickard HM. Finite-element stress analysis of the crowns of normal and restored teeth. *J Dent Res.* 1976; 55:1004–1011.
19. Middleton J, Jones M, Wilson A. The Role of the periodontal ligament in bone modeling: the initial development of a time-dependent finite element model. *Am J Orthod Dentofacial Orthop.* 1996;109:155–162.
20. Tanne K, Sakuda M, Burstone CJ. Three-dimensional finite element analysis for stress in the periodontal tissue by orthodontic forces. *Am J Orthod Dentofacial Orthop.* 1987;92:499–505.
21. McGuinness N, Willson AN, Jones M, Middleton J, Robertson NR. Stresses induced by edgewise appliances in the periodontal ligament—a finite element study. *Angle Orthod.* 1992;62:15–22.
22. *Lifecore Biomedical, Oral Restorative Division* [catalog] Chaska, Minnesota: Lifecore; 1998:6.
23. Kraus BS, Jordan ER, Abrams L. *Anatomia dental y oclusión,* 2nd ed. México: *Interamericana*; 1972:34–44.
24. Lindhe J. *Periodontología clínica,* Buenos Aires: Panamericana 1986:39.
25. Rieger MR, Adams WK, Kinzel GL, Brose MO. Finite element analysis of bone-adapted and bone-bonded endosseous implants. *J Prosthet Dent.* 1989;62:436–440.
26. Van Rossen IP, Braak LH, Putter C, Groot K. Stress-absorbing elements in dental implants. *J Prosthet Dent.* l990;64:198–205.
27. Meijer GJ, Starmans FJM, de Putter C, Van Blitterswrjk CA. The influence of a flexible coating on the bone stress around dental implants. *J Oral Rehabil.* 1995;22:105–111.
28. Storey EE, Smith R. Force in orthodontics and its relation to tooth movement. *Aust Dent J.* 1952;56:11–18.
29. Burstone CJ. The segmented arch approach to space closure. *Am J Orthod Dentofacial Orthop.* 1982;82:361–378.
30. Kuhlberg AJ, Burstone CJ. T-loop position and anchorage control. *Am J Orthod Dentofacial Orthop.* 1997;112:12–18.
31. Puente MI, Galbán L, Cobo JM. Initial stress differences between tipping and torque movements. A three-dimensional finite element analysis. *Eur J Orthod.* 1996;18:329–339.
32. Barbier L, Sloten JV, Krzeinski G, Schepers E. Finite element analysis of non axial versus axial loading of oral implants in the mandible of the dog. *J Oral Rehabil.* 1998;25:847–858.
33. Clelland NL, Ismail YH, Zaki HS, Pipko D. Three-dimensional finite element stress analysis in and around the screw-vent implant. *Int J Oral Maxillofac Implants.* 1991;6:391–392.
34. Storey E. The nature of tooth movement. *Am J Orthod.* 1973;63: 292–314.
35. Wilson AM, Middleton J. The finite element analysis of stress in the periodontal ligament when subject to vertical orthodontic forces. *Br J Orthod.* 1994;21:161–167.
36. Burstone CJ, Van Steenbergen E, Hanley KJ. *Modern Edgewise Mechanics and the Segmented Arch Technique.* Farmington, Conn: Ormco Corporation; 1995:4.